The Luminosity Function of Cluster Radio Relics

M. Brüggen[1], T.A. Enßlin[2], F. Miniati[2]

m.brueggen@iu-bremen.de

ABSTRACT

In this paper we compute the luminosity function of radio relics. In our calculation we include only those relics that are produced by the compression of former radio cocoons. This compression is provided by shocks that are generated in the process of structure formation. Starting from an analytical model for the luminosity evolution of ageing radio cocoons, the luminosity function of radio galaxies and the statistics of shocks as inferred from cosmological simulations, we are able to make the first estimates of the brightness distribution of radio relics. The computed luminosity function is consistent with current observations and predicts that more than 10^3 radio relics should be discovered with the upcoming generation of low-frequency radio telescopes. Moreover, we predict that radio relics are predominantly found in low-pressure regions outside the cores of clusters.

1. Introduction

A number of diffuse, steep-spectrum radio sources without optical identification has been observed in galaxy clusters. These sources have complex morphologies and show diffuse and irregular emission (Kempner & Sarazin 2001; Bacchi et al. 2003). They are usually subdivided into two classes, denoted as 'radio halos' and 'radio relics' (a more detailed classification scheme is put forward by Kempner et al. (2003)). Cluster radio halos are unpolarised and have diffuse morphologies that are similar to those of the thermal X-ray emission of the cluster gas. Unlike halos, radio relics are typically located near the periphery of the cluster; they often exhibit sharp emission edges and many of them show strong radio polarisation. For more details on observations of diffuse cluster radio sources the reader is referred to (Kempner & Sarazin 2001; Giovannini 1999).

[1]International University Bremen, Campus Ring 1, 28759 Bremen, Germany

[2]Max-Planck Institut für Astrophysik, Karl-Schwarzschild-Str 1, 85740 Garching, Germany

The origin of these diffuse radio sources is still not entirely clear. Two processes for the formation of radio relics have been proposed, both of which invoke the action of shock waves. Shock waves are produced in the course of structure formation, e.g. by mergers between, and accretion onto clusters of galaxies (Miniati et al. 2000), and may provide the necessary acceleration of the electrons. The two most important mechanisms that are believed to produce radio relics are: (i) in-situ diffusive shock acceleration by the Fermi I process (Enßlin et al. 1998; Roettiger et al. 1999; Miniati et al. 2001) and (ii) re-acceleration of electrons by compression of existing cocoons of radio plasma (Enßlin & Gopal-Krishna 2001; Enßlin & Brüggen 2002). In all the aforementioned scenarios the diffuse radio emission is associated with shock-fronts. Some of the relics are characterised by highly structured morphologies and those are more likely to have been produced by the compression scenario (Enßlin & Brüggen 2002). In this paper we will focus on the latter types of relics, i.e. those that are produced by compression of old radio cocoons.

When a radio ghost, an old invisible radio galaxy cocoon, is passed by a cluster merger shock wave with a typical velocity of a few 1000 km/s the ghost is compressed adiabatically and not shocked because of the much higher sound speed within it. Therefore, diffusive shock acceleration is unlikely to be the prime mechanism that re-energises the relativistic electron population. However, it has been shown that the energy gained during the adiabatic compression, together with the increase in the magnetic fields strength, can cause the old radio cocoon to emit radio waves again. Enßlin & Gopal-Krishna (2001) showed that the spectra thus produced are consistent with an old electron population that has been adiabatically compressed. With the aid of magneto-hydrodynamical simulations Enßlin & Brüggen (2002) demonstrated that the resulting relics typically possess a toroidal shape and are partially polarised - in good agreement with observations.

In this paper we attempt to predict the radio-luminosity function of cluster radio relics, in particular of radio relics that are produced via compression of old radio plasma [3]. Our predictions are intended to provide an order-of-magnitude estimate for the potential detection of diffuse radio sources by future high-sensitivity radio observatories, such as the LOw Frequency ARray (LOFAR) and the Square Kilometer Array. It is too early to aim for great precision in this calculation. Here, we merely attempt to devise a simple and physically intuitive model which will give a first estimate of the luminosity function. The paper is organised as follows: In the following section we explain conceptually our approach in calculating the radio relic luminosity function. In Sec. III we describe the cosmological simulations that provide the input for our calculations, which then are presented in detail in Sec. IV. Finally,

[3]Recently, a new nomenclature has been proposed where this type of relic is called 'radio phoenix'.

the results are presented and discussed in Sec. V.

2. Outline

The progenitors for radio relics are so-called 'radio ghosts', which are radio-quiet bubbles of non-thermal plasma released by formerly active radio galaxies. In the picture of relic formation considered here, the 'ghost' bubbles are re-energised by compression by large-scale shocks. Consequently, for a calculation of the relic luminosity function, we have to determine the statistics of, both, the relevant properties of radio ghosts and of cosmic shock waves.

Radio ghosts:
In order to calculate the statistics of radio ghosts, we start from the luminosity distribution of radio galaxies that form the progenitors of radio ghosts. In the next step, the observed radio galaxy luminosity function needs to be translated into a birth rate of radio ghosts, and this is done by assuming a constant lifetime for the radio galaxy of $t_{\rm bubble} \sim 10^7$ yrs. This means that the radio cocoon is observable on average for $\sim 10^7$ yrs.

This step is a coarse simplification since it ignores any intrinsic luminosity evolution during the observable lifetime of a radio galaxy (Kaiser & Cotter 2002; Blundell & Rawlings 2000; Kaiser & Alexander 1997; Kaiser et al. 1997). Its justification lies partially in the fact that a more sophisticated treatment would require the introduction of several poorly constrained parameters, an expense which is not rewarded by the only moderate gain in accuracy. The observed radio luminosity function is dominated by the long-lasting late stage in the evolution of radio galaxies in which the radio luminosity is nearly constant. Therefore, the approximation that each source only has a single luminosity during its lifetime is acceptable compared to other uncertainties.

Now, the luminosity of a radio ghost is boosted when it is compressed by a shock wave. Whether this leads to an observable radio relic depends on a combination of shock strength and age of the radio ghost. The shock has to be strong enough to lead to a sufficient amplification of the magnetic field inside the ghost and to a sufficient increase of the energies of the most relativistic electrons. Only a strong enough shock allows the renewed emission of synchrotron emission at observable frequencies. However, the maximal energy in the electron spectrum decreases with age owing to the unavoidable synchrotron and CMB inverse-Compton energy losses. This implies that the radio ghost must not exceed a certain age, if it is to be re-activated by a shock wave of a given strength, and, therefore, we need to estimate the age distribution of radio ghosts.

The birth rate of radio ghosts changes drastically during cosmological times, as we know from the strongly redshift-dependent radio luminosity function. However, on the timescale of $\sim 10^8$ yrs, over which radio ghosts are able to be re-activated by typical shock waves, the radio luminosity function is roughly constant. Therefore, instead of modelling the demographic evolution of the ghost distribution, for simplicity we use a flat age distribution, even though Kaiser & Alexander (1999) do not fully confirm this approximation. This implies that the number of ghosts is given by

$$\dot{N}_{\rm ghost} = \frac{N_{\rm rgal}}{t_{\rm bubble}}. \tag{1}$$

In the next step, the maximal age, within which a radio ghost can be re-activated, is calculated. Because of the very low density inside the radio cocoon, inverse Compton and synchrotron emission are the dominant processes whereby the electrons lose their energy. Thus, the maximal Lorentz factor of the relativistic electron population evolves according to

$$\frac{d\gamma_{\rm max}}{dt} = -a_0 \left(\epsilon_B + \epsilon_{\rm CMB}\right) \gamma_{\rm max}^2 \,, \tag{2}$$

where ϵ_B and $\epsilon_{\rm CMB}$ are the magnetic field and CMB energy densities respectively, and $a_0 = \frac{4}{3}\,\sigma_{\rm T}/(m_{\rm e}\,c)$. This equation has the solution

$$\gamma_{\rm max}(t) = \left(\frac{1}{\gamma_{\rm max}(t_0)} + a_0 \left(\epsilon_B + \epsilon_{\rm CMB}\right) (t - t_0) \right)^{-1} \,, \tag{3}$$

for a period t_0 to t with constant ambient conditions (ϵ_B, $\epsilon_{\rm CMB}$ = const). A shock wave of Mach number M compresses radio plasma with a relativistic equation of state (adiabatic index of $\frac{4}{3}$) by a factor

$$C = C(M) = \left(\frac{5M^2 - 1}{4} \right)^{3/4} \tag{4}$$

and thereby increases the maximum electron energy adiabatically to $\gamma_{\rm max,2} = \gamma_{\rm max,1} C^{\frac{1}{3}}$ and the magnetic field energy density to $\epsilon_{B_2} = \epsilon_{B_1} C^{\frac{4}{3}}$, where the index 1 and 2 labels pre- and post-shock quantities respectively. For simplicity, radiative energy losses during the short compression phase are neglected. The radio ghost can be regarded to be reactivated, and therefore to form a radio relic , if the characteristic synchrotron frequency of the most energetic electrons

$$\nu_{\rm max,2} = \frac{3\,e\,B_2}{2\,\pi\,m_{\rm e}\,c}\,\gamma^2_{\rm max,2} \tag{5}$$

is above the observing frequency ν. The relic remains visible for a period t_2 until (the now enhanced) radiative cooling according to Eqs. 2 and 3 has moved the synchrotron cut-off frequency below ν.

Clearly, in order to compute the synchrotron ageing, we need a description of the magnetic field strength inside the radio ghosts. Here, we assume that the magnetic energy density is some fraction of the total pressure inside the ghost, which itself is in pressure equilibrium with the ambient pressure p. Hence, we need to specify the distribution of radio ghosts as a function of the ambient pressure, which we approximate as follows:

Our starting point is the spatial statistics of the radio galaxy distribution, which we scale with some power α of the ambient gas density ρ. We assume that the radio galaxy distribution $N_{\rm rgal}(L, \vec{r}, z)$ per luminosity and for a specific volume element at location $\vec{r}$ can be written as a direct product of its global luminosity function $N_{\rm rgal}(L, z)$ and a term proportional to ρ^α (for a discussion see Kaiser & Alexander (1999)). This allows us to construct the radio luminosity function as the number of radio galaxies of luminosity $L = L(\nu)$ per unit volume V, pressure p and luminosity as a function of p, L and redshift z

$$N_{\rm rgal}(L, p, z)\ dp\ dV\ dL = \mathcal{D}(L, z) R_\alpha(p)\ dp\ dV\ dL\ . \tag{6}$$

One can get a handle on α by demanding that $\sim$ 30 % - 50 % of all radio galaxies lie in clusters (Ledlow & Owen 1995, 1996). If we characterise clusters by means of their pressures, i.e. as environments where the pressure lies above $\sim 10^{-12}$ erg cm^{-3}, we find that for α of around 1.5 about 30 % of radiogalaxies should lie in clusters and for $\alpha = 2$ about 60 % would lie in clusters. One should note, however, that these estimates are very crude and should be treated with caution. So in the following, we will present our results for these two values of α.

The distribution function $R_\alpha(p)$ is defined via

$$R_\alpha(p')dp' = \frac{A}{V} dp' \int dV\ \rho(\mathbf{r})^\alpha \delta(p(\mathbf{r}) - p')\ , \tag{7}$$

where δ is the delta function and A is a normalisation constant chosen such that $\int dp\ R_\alpha(p) = 1$.

As explained in more detail later, $R_\alpha(p)$ is extracted from a simulation of cosmological structure formation. Now we can also express the birth rate of radio *ghosts* per unit p, L

and V

$$\dot{N}_{\rm ghost}\ dp\ dV\ dL = \frac{N_{\rm rgal}}{t_{\rm bubble}}\ dp\ dV\ dL. \tag{8}$$

Shock waves:
When the radio ghost is compressed adiabatically, its synchrotron luminosity, L_2, increases with respect to its initial luminosity, L_1, by a factor $L_2/L_1 = [(5M^2-1)/4]^{5/2}$ (Enßlin & Gopal-Krishna 2001). This treatment ignores subtle spectral steepening effects that occur when the spectral cut-off passes the observing frequency[4], and the detailed shape of the synchrotron emission spectral kernel. However, our simplified treatment should be entirely sufficient for our purposes.

Finally, we need to determine the frequency with which shock waves of a given Mach number M sweep over a radio ghost, which is situated at redshift z in an environment of pressure p. This frequency is written as

$$\omega(p, M, z)\ dM = \frac{\dot{m}^\alpha(p, M, z)}{R_\alpha}\ dM\ , \tag{9}$$

where $\dot{m}^\alpha$ is the flow of ρ^α (a density-biased mass flow) integrated over shocks of Mach number M, at redshift z and in an environment of pressure p, given by

$$\dot{m}^\alpha(p, M, z) = \frac{1}{V}\int d\mathbf{A}_{\rm shock}\cdot\mathbf{v}_{\rm shock}\ \rho(\mathbf{r})^\alpha\ \delta(M - v_{\rm shock}/c_s)\delta(p - \rho c_s^2/\gamma_{\rm gas})\ , \tag{10}$$

where V is the volume considered, c_s the sound speed, $\mathbf{v}_{\rm shock}$ the shock velocity and $\gamma_{\rm gas} = \frac{5}{3}$ the adiabatic index of the gas. Note that p, ρ and c_s are evaluated ahead of the shock.

It is useful to define the time between successive shocks of any strength, which is given by

$$\tau(p, z) = \left[\int_0^\infty dM\ \omega(p, M, z)\right]^{-1}. \tag{11}$$

---

[4]The aging of the relativistic electron populations, which was originally a power-law in Lorentz-factor γ with a spectral index $\alpha_{\rm e}$

$$f(\gamma, t_1 = 0)\, d\gamma = f_0\, \gamma^{-\alpha_{\rm e}}\, d\gamma\,,$$

is described by

$$f(\gamma, t_1)\, d\gamma = f_0\, \gamma^{-\alpha_{\rm e}}\, (1 - \gamma/\gamma_{\rm max}(t_1))^{\alpha_{\rm e}-2}\theta(\gamma_{\rm max} - \gamma)\, d\gamma$$

which shows a spectral steepening shortly below the cutoff for $\alpha_{\rm e} > 2$.

From the simulations that will be described in the following section, this time was inferred to be of the order of 3 Hubble times, which is roughly consistent with the findings by (Cen & Ostriker 1999), who claim that about 30 % of the baryons in the universe at redshift zero have been shocked. We also find that τ increases with pressure which is attributed to the fact that there are many more low-pressure regions in the universe and that these regions have lower sound speeds and shock more easily.

3. Numerical Simulation of the Large Scale Structure

The formation and evolution of the large-scale structure is computed by means of an Eulerian, grid based Total-Variation-Diminishing hydro+N-body code (Ryu et al. 1993).

We adopt a canonical, flat ΛCDM cosmological model with a total mass density $\Omega_m = 0.3$ and a vacuum energy density $\Omega_\Lambda = 1 - \Omega_m = 0.7$. We assume a normalized Hubble constant $h \equiv H_0/100$ km s^{-1} Mpc$^{-1} = 0.67$ and a baryonic mass density, $\Omega_b = 0.04$. The simulation is started at redshift $z \simeq 60$ with initial density perturbations generated as a Gaussian random field and characterized by a power spectrum with a spectral index $n_s = 1$ and "cluster-normalization" $\sigma_8 = 0.9$. We adopt a computational box size of $50\,h^{-1}$ Mpc. In this box the dark matter component is described by 256^3 particles whereas the gas component is evolved on a comoving grid of 512^3 zones. Thus each numerical cell measures about $100\,h^{-1}$ kpc (comoving) and each dark matter particle corresponds to $2 \times 10^9\,h^{-1}\,M_\odot$. Further details on the cosmological simulations can be found in Miniati (2002).

The results from the simulation are used to build the distribution functions $\dot{m}_\alpha$ and R_α that are required in our calculations. As in previous studies (Miniati et al. 2000), we identify shocks as converging flows ($\nabla \cdot \mathbf{v} < \mathbf{0}$) that experience a pressure jump $\Delta P/P$ above a threshold corresponding to a Mach number M=1.5. Once a shock has been identified the jump conditions are evaluated from the numerical solution. Finally, the shock speed and Mach number are computed Landau & Lifshitz (1987).

4. Calculations

In this section we carry out the calculations that were outlined in prose in the previous sections. The total number of radio *relics* of luminosity L_2 per unit volume at a given redshift is given by the birth rate of radio *ghosts*, $\dot{N}_{\rm ghost}$, times the time for which the radio relic is visible, t_2, times the frequency of shocks of given strength, ω that can boost their luminosity from L_1 to L_2. All this is integrated over the luminosity of the *ghosts*, L_1, the

age of the *ghost* at the time of compression, t_1, and pressure and Mach number, i.e.

$$\begin{aligned} N_{\rm relic}(L_2,z) &= \int dt_1 \int dL_1 \int dp \int dM\ \dot{N}_{\rm ghost}(L_1,p,z) t_2(t_1,p,M,z) \\ &\quad \omega(p,M,z) e^{-t_1/\tau} \delta[L_2 - ((5M^2-1)/4)^{5/2} L_1], \end{aligned} \tag{12}$$

where τ is given by Eq.(11) and $t_2(t_1,p,M,z)$ the time for which the relic is visible, i.e., until the cut-off frequency falls below the observing frequency. This time is calculated below. Note that we have introduced a factor of $e^{-t_1/\tau}$ which ensures that a radio ghost can only be reactivated once.

We can perform the integration with respect to L_1, by assuming that, upon compression, the luminosity of the radio ghosts increases by

$$\frac{L_2}{L_1} = \left(\frac{p_2}{p_1}\right)^{5/2} = \left(\frac{5M^2-1}{4}\right)^{5/2} =: g(M), \tag{13}$$

where L_2 and L_1 and p_2 and p_1 refer to the post-/pre-shock luminosities and pressures, respectively. Moreover, in concordance with observations, a spectral index of 1 for the synchrotron emission was assumed (Enßlin & Brüggen 2002). Note that we make the simplifying assumption that the ghost instantaneously flares up to L_2 as the shock sweeps by. Performing the L_1-integration, we obtain

$$N_{\rm relic}(L_2,z) = \int dp \int dM\ \dot{N}_{\rm ghost}(L_2/g(M),p,z) \frac{\omega(p,M,z)}{g(M)} \int dt_1\ t_2(t_1,p,M,z) e^{-t_1/\tau}\ . \tag{14}$$

The 'visibility time' t_2 is calculated as follows: The cut-off frequency, ν_c, decreases due to synchrotron radiation and Compton scattering with the CMB photons. Furthermore, the compression of the radio ghost after a time t_1 boosts the cut-off frequency by a factor of $(p_2/p_1)^{1/2}$. Hence, ν_c is given by

$$\nu_c = \frac{3eB_2}{2\pi m_e c a_0^2} \left[\left(\frac{p_2}{p_1}\right)^{-1/4} (\epsilon_{B_1} + \epsilon_{\rm CMB}) t_1 + (\epsilon_{B_2} + \epsilon_{\rm CMB}) t_2 \right]^{-2}, \tag{15}$$

where $B_2 = B_1 (p_2/p_1)^{1/2}$ is the magnetic field strength in the ghost after compression (note that $B_1 = \sqrt{\eta_{\rm B} 8\pi p_1}$), $\epsilon_{\rm CMB}$ the energy density of the CMB (4.02×10^{-13} erg cm^{-3} at $z=0$) and $a_0 = \frac{4\sigma_{\rm T}}{3 m_e c}$. Here, we assumed that the magnetic energy density is some fraction of the total pressure in the ghost $\eta_{\rm B} \approx 0.3$.

Solving for t_2 yields:

$$t_2 = \left[\left(\frac{3eB_2}{2\pi m_e c a_0^2 \nu} \right)^{1/2} - \left(\frac{p_2}{p_1} \right)^{-1/4} (\epsilon_{B_1} + \epsilon_{\rm CMB}) t_1 \right] / (\epsilon_{B_2} + \epsilon_{\rm CMB}) \ . \tag{16}$$

Now we calculate the last integral in Eq. (14), i.e. $I = \int dt_1 \ t_2 \exp(-t_1/\tau)$, where it is convenient to introduce the definitions for the maximal 'life time' of the relic:

$$t_{\rm max} = \frac{1}{\epsilon_{B_2} + \epsilon_{\rm CMB}} \left(\frac{3eB_1}{2\pi m_e c a_o^2 \nu} \right)^{1/2} \left(\frac{5M^2 - 1}{4} \right)^{1/2} \ , \tag{17}$$

and the ratio of the loss rates before and after compression:

$$r = \frac{\epsilon_{B_1} + \epsilon_{\rm CMB}}{\epsilon_{B_2} + \epsilon_{\rm CMB}} \ . \tag{18}$$

Now the integral, I, reduces to:

$$I = (p_2/p_1)^{-1/4} \int_0^{t_{\rm max}/r} dt_1 \ (t_{\rm max} - r t_1) \exp(-t_1/\tau) \ , \tag{19}$$

which can be written as

$$I = (p_2/p_1)^{-1/4} [r\tau t_{\rm max} e^{-t_{\rm max}/r\tau} + (\tau t_{\rm max} - r\tau^2)(1 - e^{-t_{\rm max}/r\tau})] \tag{20}$$

or

$$I = \left(\frac{5M^2 - 1}{4} \right)^{-1/4} [\tau t_{\rm max} - r\tau^2 (1 - e^{-t_{\rm max}/r\tau})] \ , \tag{21}$$

where r and $t_{\rm max}$ are functions of p, M, z and τ a function of p and z.

Hence the number of radio relics per unit volume is given by the integral:

$$N_{\rm relic}(L_2, z) = \int dp \int dM \ \dot{N}_{\rm ghost}(L_2/g(M), p, z) I(p, M, z) \omega(p, M, z)/g(M) \tag{22}$$

$$\begin{aligned} N_{\rm relic}(L_2, z) \ &= \ \int dp \int dM \ \dot{N}_{\rm ghost}(L_2/g(M), p, z) \left(\frac{5M^2 - 1}{4} \right)^{-11/4} \omega\tau \\ &\quad [t_{\rm max} - r\tau(1 - e^{-t_{\rm max}/r\tau})] \ . \end{aligned} \tag{23}$$

For the radio luminosity function we used 'model A' from Willott et al. (2001):

$$\mathcal{D}(L,z) = \rho_{\rm l} + \rho_{\rm h} \ , \tag{24}$$

where

$$\rho_{\rm l} = \rho_{\rm lo} \left(\frac{L}{L_{\rm l\star}}\right)^{-\alpha_{\rm l}} \exp\left(\frac{-L}{L_{\rm l\star}}\right)(1+z)^{k_{\rm l}} \qquad \text{for } z < z_{\rm lo}, \tag{25}$$

$$\rho_{\rm l} = \rho_{\rm lo} \left(\frac{L}{L_{\rm l\star}}\right)^{-\alpha_{\rm l}} \exp\left(\frac{-L}{L_{\rm l\star}}\right)(1+z_{\rm lo})^{k_{\rm l}} \quad \text{for } z \geq z_{\rm lo}, \tag{26}$$

$$\rho_{\rm h} = \rho_{\rm ho} \left(\frac{L}{L_{\rm h\star}}\right)^{-\alpha_{\rm h}} \exp\left(\frac{-L_{\rm h\star}}{L}\right) f_{\rm h}(z). \tag{27}$$

The high–luminosity evolution function $f_{\rm h}(z)$ takes the form:

$$f_{\rm h}(z) = \exp\left\{-\frac{1}{2}\left(\frac{z-z_{\rm ho}}{z_{\rm h1}}\right)^2\right\} \ , \tag{28}$$

where the different parameters for this model are given in Table 1. Finally, the remaining two integrals over p and M in Eq. 23 will have to be done numerically.

5. Results and Discussion

The number density of relics per decade in luminosity is shown in Fig. 1. Between $L = 10^{20}$ and 10^{29} W Hz^{-1} sr^{-1} the number or radio relics per unit volume follows a power law $N \propto L^{\beta}$ with $\beta = -0.6$. As indicated in the plot the number density of relics goes down with increasing redshift.

The number of relics per decade in brightness at 150 MHz as a function of flux is shown in Figs. 2 and 3 for $\alpha = 1.5$ and 2, respectively. Their distribution roughly follows a power law of index -0.6. For higher values of α the number of relics decreases because, for higher α, a larger fraction of radio ghosts is concentrated in the cores of clusters, where the lifetime of the radio ghosts is shorter and the chances for a reappearance as a radio relics diminish. The number of radio relics at 151 MHz is higher than the number of *radio halos* at 1.4 GHz by a factor of ~ 10 as predicted by Enßlin & Röttgering (2002). Assuming a spectral index of 1, as we did in this paper, this would imply that the numbers of radio relics and halos should roughly match if compared at the same frequency, which is what is indeed found. In Fig. 2 we have included a histogram with the observed flux density distribution of the sample of Feretti (1999). Even though the current sample of radio relics is still poor, we find that

current observations are not inconsistent with our predictions. Ignoring the uncertainties of our model, one would conclude from Figs. 2 and 3 that, in the range between 1 and 10 Jansky, approximately 10 % of the radio relics have been detected. However, we fear that the predicted number may be a bit high and that we have overestimated the luminosities due to two reasons: First, we neglected the enhanced cooling during the compression of the bubble and, second, the majority of radio cocoons will not be in exact pressure equilibrium but are more likely to be still somewhat overpressured when they are being compressed. These two effects will shift the curves to the left while leaving the slope unchanged.

In order to determine in which environments the majority of relics is to be found, we computed the contribution to the total flux density from relics that lie within a certain pressure range (since pressure is the free variable in our formalism). The solid line in Fig. 2 corresponds to the total number of relics, while the dashed line includes only the contribution from relics that are found at pressures $p > 10^{-14}$ g cm^{-3}, the dotted line to those at $p > 10^{-13}$ g cm^{-3}, and the dot-dashed line only those at $p > 10^{-12}$ g cm^{-3}. We find that the majority of radio relics is found at pressures between a bit below 10^{-14} g cm^{-3} and 10^{-13} g cm^{-3}, which are typical values for pressures at the edges of galaxy cluster. This is in good agreement with the observed locations of radio relics: nearly all of them have been found in the periphery of galaxy clusters. However, similar pressure conditions are also encountered around groups and in filaments of galaxies, where we would also expect that future high-sensitivity observations detect radio relics. Conversely, in the cores of clusters, i.e. at typical pressures of $p < 10^{-12}$ g cm^{-3}, only $\sim 1\%$ of radio relics are expected (see dot-dashed line). The fact, that shocks become stronger when they leave the cluster, more than makes up for the fact that there are fewer radio galaxies in the outer regions. Moreover, radio plasma is very short-lived at high ambient pressures because the synchrotron losses are high. Thus, even though there is more radio plasma in the cores of clusters, only little of it is fresh enough to form radio relics again. Here we predict that radio relics are predominantly found in low-pressure regions outside the cores of clusters.

Using very simple assumptions we were able to give a first gross estimate of the number of radio relics that are expected at different flux limits. Upcoming low-frequency radio telescopes such as LOFAR are ideally suited to search for relics at the edges of clusters. LOFAR is expected to have a point source sensitivity of 0.13 mJy at 120 MHz within one hour of integration time and a 4 MHz bandwidth. A survey covering half the sky can be accomplished in a years timescale at this frequency and with this depth (Enßlin & Röttgering 2002). Such a survey is likely to find of the order of 10^4 radio relics. As mentioned earlier, we believe that this number may be a bit too high because the number of detected relics between 1 and 10 Jansky is lower by a factor of roughly 10. However, given the simplicity of our model and the scarceness of data, this is not a bad match. More importantly, while

the normalisation of the brightness distribution is sensitive to some of our assumptions and, consequently, somewhat uncertain, both, the slope of the distribution and the relative contributions from different pressure bins are fairly robust predictions.

Finally, let us summarise the assumptions that went into the calculation of the radio relics luminosity function:

(i) Radio relics are produced by the adiabatic compression of fossil radio plasma (radio ghosts).

(ii) The birth rate of radio ghosts is given by the number of radio galaxies divided by a constant activity time span, $t_{\rm bubble}$.

(iii) The number density of radio galaxies is given by the radio luminosity function (Willott et al. 2001) scaled with a power of the local density. This power was assumed to be either 1.5 or 2.

(iv) The compression of the radio plasma is instantaneous upon passage of a shock.

(v) No stochastic particle reacceleration takes place and magnetic fields are merely passive (magnetic energy density = 0.3 of total pressure).

(vi) Within the time within which the radio ghosts can be reactivated, they do not migrate (by buoyancy or advection).

We thank M. Hoeft for valuable discussions. MB thanks the Max-Planck Insitut für Astrophysik in Garching for their kind hospitality. FM acknowledges support by the Research and Training Network "The Physics of the Intergalactic Medium" under EU contract HPRN-CT2000-00126 RG29185.

Model	$\log(\rho_{\rm lo})$	$\alpha_{\rm l}$	$\log(L_{\rm l\star})$	$z_{\rm lo}$	$k_{\rm l}$	$\log(\rho_{\rm ho})$	$\alpha_{\rm h}$	$\log(L_{\rm h\star})$	$z_{\rm ho}$	$z_{\rm h1}$
A	−7.503	0.584	26.46	0.710	3.60	−6.740	2.42	27.42	2.23	0.642

Table 1: Parameters chosen for the radio luminosity function (Model A from Willott et al. (2001)).

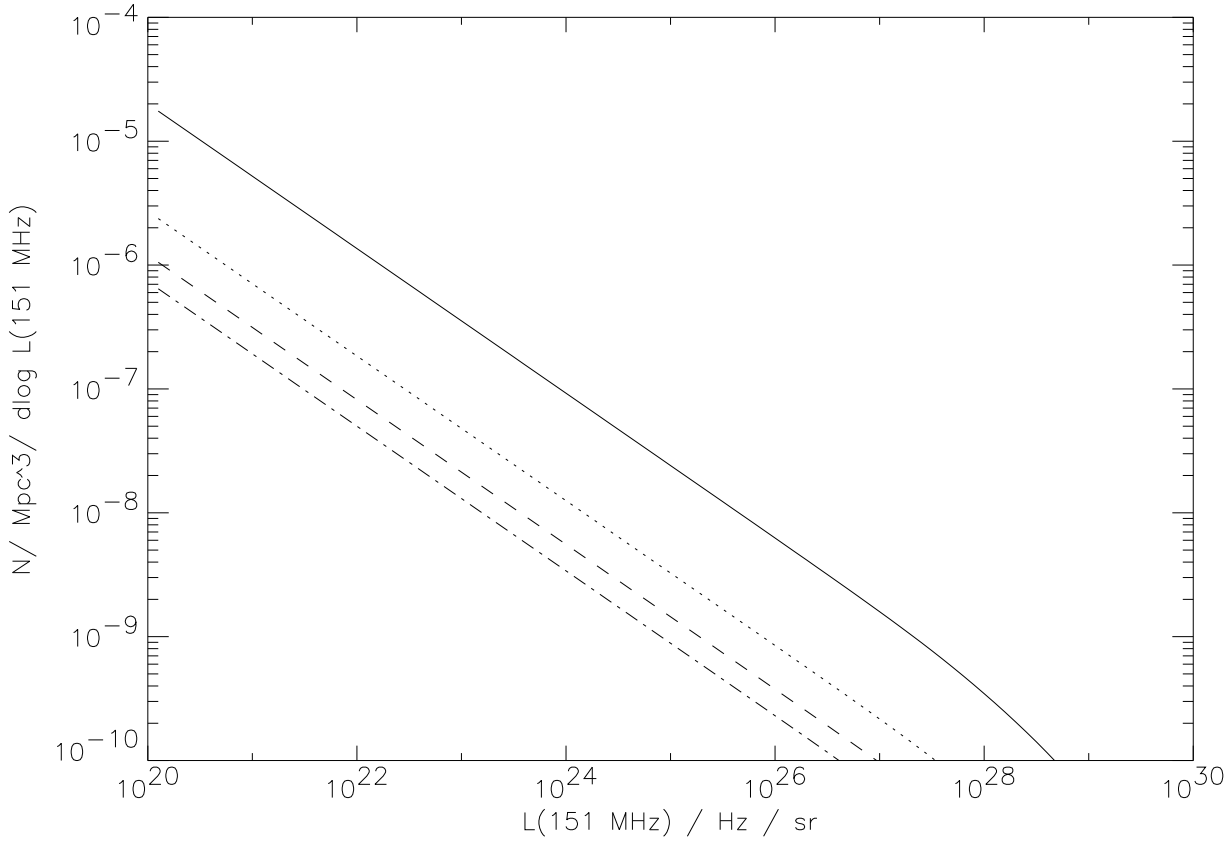

Fig. 1.— Radio relic luminosity function at 151 MHz for $\alpha = 2$ at $z = 0.001$ (solid), 0.75 (dotted), 1.5 (dashed) and 3 (dot-dashed).

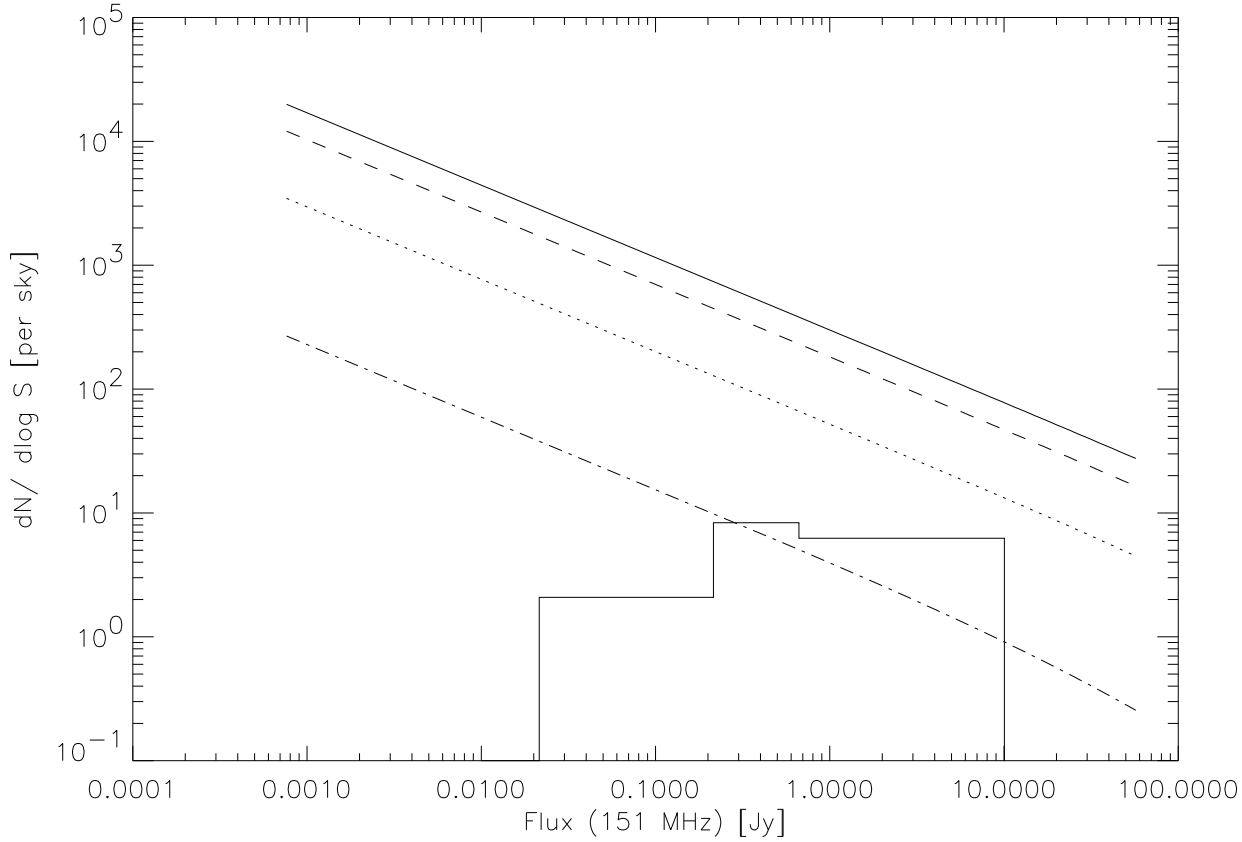

Fig. 2.— Expected brightness distribution for radio halos at 151 MHz (assumed $h = 0.7$, $\Omega_m = 0.3$). The solid line corresponds to the total number of relics, while the dashed line includes only the contribution from relics that are found at pressures $p > 10^{-14}$ g cm^{-3}, the dotted line to those at $p > 10^{-13}$ g cm^{-3}, and the dot-dashed line only those at $p > 10^{-12}$ g cm^{-3}. Here α was taken as 1.5.

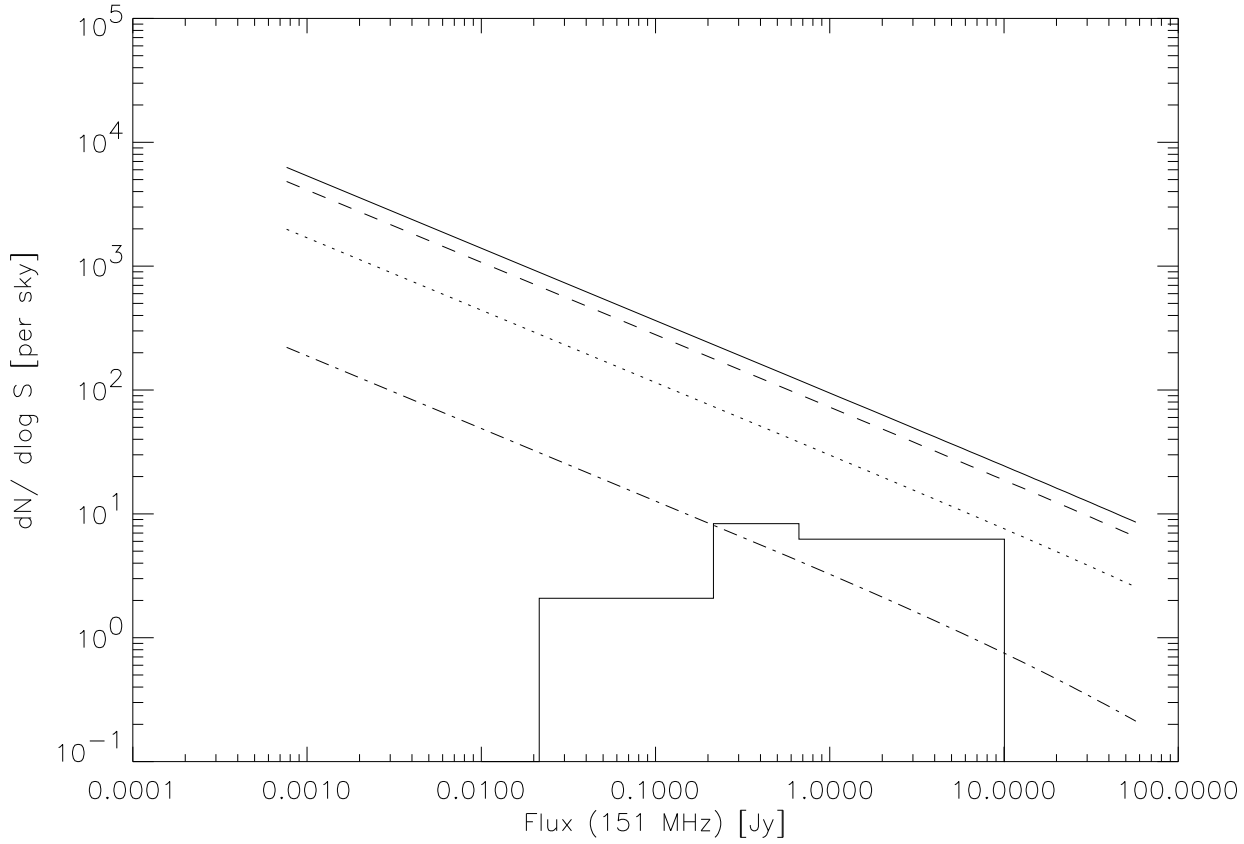

Fig. 3.— Same as Fig. 2 except that here α was taken as 2.

Cluster	z	$P_{1.4}[10^{23}$ W/Hz]	L.S.[Mpc]	$L_{Xbol}[10^{44}$ erg/s]	T[keV]	d [Mpc]
A85	0.0555	6.26	0.48	19.52	5.1	0.54
A115	0.1971	255.5	1.88	31.09	4.9	0.93
A610	0.0956	7.65	0.57	-	-	0.71
A1300	0.3071	92.4	0.95	47.63	10.5	0.80
A1367	0.0216	0.71	0.29	2.87	3.5	0.83
A1656	0.0232	7.03	1.17	20.42	8.2	2.72
A2255	0.0809	3.51	0.98	12.42	5.4	1.23
A2256	0.0581	4.48	1.11	18.39	7.5	0.59
A2744	0.3080	74.3	1.84	62.44	11.0	1.91
A3667	0.0552	323.1	2.63	22.70	7	2.45

Table 2: Col. 1: cluster name; Col. 2: cluster redshift; Col. 3: radio power of the diffuse source at 1.4 GHz; Col. 4: largest linear size of the diffuse source; Col. 5: cluster X-ray bolometric luminosity; Col 6: cluster temperature obtained by averaging values in the literature; Col. 7: projected distance of the diffuse source from the cluster centre (from Feretti (1999))

REFERENCES

Bacchi, M., Feretti, L., Giovannini, G., & Govoni, F. 2003, A&A, 400, 465

Blundell, K. M. & Rawlings, S. 2000, AJ, 119, 1111

Cen, R. & Ostriker, J. P. 1999, ApJ, 514, 1

Enßlin, T. A., Biermann, P. L., Klein, U., & Kohle, S. 1998, A&A, 332, 395

Enßlin, T. A. & Brüggen, M. 2002, MNRAS, 331, 1011

Enßlin, T. A. & Gopal-Krishna. 2001, A&A, 366, 26

Enßlin, T. A. & Röttgering, H. 2002, A&A, 396, 83

Feretti, L. 1999, in Diffuse Thermal and Relativistic Plasma in Galaxy Clusters, 3

Giovannini, G. 1999, in Diffuse Thermal and Relativistic Plasma in Galaxy Clusters, 13–+

Kaiser, C. R. & Alexander, P. 1997, MNRAS, 286, 215

—. 1999, MNRAS, 302, 515

Kaiser, C. R. & Cotter, G. 2002, MNRAS, 336, 649

Kaiser, C. R., Dennett-Thorpe, J., & Alexander, P. 1997, MNRAS, 292, 723

Kempner, J. C., Blanton, E. L., Clarke, T. E., Enßlin, T. A., Johnston-Hollitt, M., & Rudnick, L. 2003, in The Riddle of Cooling Flows in Galaxies and Clusters of Galaxies, eds. T.H. Reiprich, J.C. Kempner and N. Soker, 0

Kempner, J. C. & Sarazin, C. L. 2001, ApJ, 548, 639

Landau, L. D. & Lifshitz, E. M. 1987, Course of Theoretical Physics, Vol. 6, Fluid Mechanics (Oxford: Pergamon Press)

Ledlow, M. J. & Owen, F. N. 1995, AJ, 109, 853

—. 1996, AJ, 112, 9

Miniati, F. 2002, MNRAS, 337, 199

Miniati, F., Jones, T. W., Kang, H., & Ryu, D. 2001, ApJ, 562, 233

Miniati, F., Ryu, D., Kang, H., Jones, T. W., Cen, R., & Ostriker, J. P. 2000, ApJ, 542, 608

Roettiger, K., Burns, J. O., & Stone, J. M. 1999, ApJ, 518, 603

Ryu, D., Ostriker, J. P., Kang, H., & Cen, R. 1993, ApJ, 414, 1

Willott, C. J., Rawlings, S., Blundell, K. M., Lacy, M., & Eales, S. A. 2001, MNRAS, 322, 536